ISSN 1063-7761, Journal of Experimental and Theoretical Physics, 2015, Vol. 121, No. 6, pp. 1096–1103. © Pleiades Publishing, Inc., 2015.
Original Russian Text © A.H. Gevorgyan, 2015, published in Zhurnal Eksperimental'noi i Teoreticheskoi Fiziki, 2015, Vol. 148, No. 6, pp. 1248–1256.

STATISTICAL, NONLINEAR, AND SOFT MATTER PHYSICS

Optical Properties of a Stack of Cholesteric Liquid Crystal and Isotropic Medium Layers

A. H. Gevorgyan

Yerevan State University, ul. A. Manukyana 1, Yerevan, 025 Armenia
Institute of Applied Problems in Physics, Yerevan, 0014 Armenia
e-mail: agevorgyan@ysu.am

Received June 23, 2015

Abstract—Some new optical properties of a stack consisting of cholesteric liquid crystal (CLC) and isotropic medium layers are studied. The problem is solved by the modified Ambartsumyan method for the summation of layers. Bragg conditions for the photonic band gaps of the proposed system are presented. It is shown that the choice of proper sublayer parameters can be used to control the band structure of the system. In the general case, the effect of full suppression of absorption, which is observed in a finite homogeneous CLC layer, is not detected in the presence of anisotropic absorption in CLC sublayers. It is shown that this effect can be generated in the system under study if certain conditions are imposed on the isotropic sublayer thickness. Under these conditions, the maximum photonic density of states (PDS) increases significantly at the boundaries of the corresponding band. The influence of a change in the CLC sublayer thickness and the system thickness on PDS is investigated.

DOI: 10.1134/S1063776115120122

1. INTRODUCTION

Photonics, i.e., the science that deals with the fundamental and applied problems of generation, emission, transmission, modulation, switching, amplification, detection/probing, and processing of light signal, is being extensively developed. Photonics is an analog of semiconductor electronics, which uses photons instead of electrons to transmit signals and deals with photonic processes of processing signals. It is characterized by high data transmission rates and very low energy losses and, hence, can have the possibility of a high operation speed and miniaturization. However, electrons have a charge and can be controlled by (electric, magnetic, etc.) fields, whereas photons can only be controlled by changing medium parameters. Therefore, interest in creating new media, in particular, photonic crystals (PCs) and metamaterials with controlled parameters, has quickened in recent years.

Based on the aforesaid, PCs and metamaterials can be divided into the following two groups: solid PCs and metamaterials that are characterized by an improper elasticity and controllability by external fields, which substantially restricts their application (once created, the parameters of these media can hardly be changed), and so-called soft PCs and metamaterials. The well-known representatives of soft PCs are cholesteric liquid crystals (CLCs) and blue phases. Apart from the ability of self-organization of its periodic photonic structure, CLCs have the properties of wide-scale easy deformability, high sensitivity, and highly elastic ability of phase or morphology modulation. These properties explain the fact why such structures with a photonic band gap (PBG) rapidly react to external actions. Moreover, CLCs have the following unique optical properties: they only have a first-order PBG (for normal incidence of light) for light with circular polarization having the sense of rotation that is identical to the sign of medium chirality, and absorption and emission in CLCs also have polarization peculiarities [1, 2]. The effect of anomalously strong (anomalously weak) absorption (emission) takes place outside PBG, near its boundaries, during anisotropic absorption (amplification).

On the other hand, the soft character of CLCs limits the possibility of creating cells with a homogeneous spiral structure with $N = d/p > 10$ or more, where d is the thickness and p is the pitch of CLC helix. However, thick cells are necessary to form an ideal PBG, which is important for some applications.

To form systems with a high elasticity, easy deformability, and a high sensitivity as compared to an ideal periodic structure at a large thickness, we can use a stack of CLC and isotropic medium layers, in particular, isotropic layers subjected to specific treatment to produce homogeneous CLC sublayers. The authors of [3–11] studied the optical properties of such a stack and showed that, in contrast to a homogeneous CLC layer, this system has a higher-order PBG, and such systems can be applied in many fields, such as the production of monitors, due to multicolor reflection.

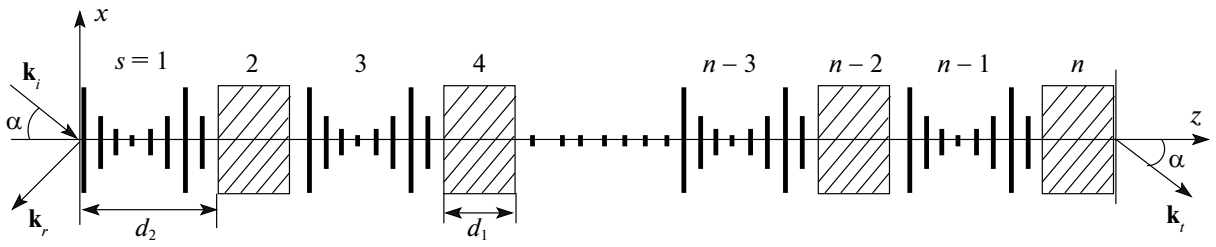

Fig. 1. Schematic diagram of a stack consisting of CLC and isotropic medium layers.

PBGs of the following two types are present in each order of reflection: incident-light-polarization selective and nonselective PBGs. Central PBG is independent of the polarization of incident light, and short-wavelength PBG has left-hand circular polarization. In other words, it appears when left-hand circular polarization light is incident on a system, and long-wavelength PBG appears for right-hand circular polarization light. In this case, the spirals in CLC sublayers are assumed to be right-handed.

However, such systems lose many useful properties of a homogeneous CLC layer (see below). In this work, we studied new properties of such a system and showed that, under certain resonance conditions, this system can exhibit all well-known and useful properties of both a homogeneous CLC layers and a stack consisting of CLC layers and an isotropic medium. Here, certain conditions are only imposed on the thickness of isotropic sublayers.

2. RESULTS AND DISCUSSION

The problem of light propagation through a stack consisting of CLC and isotropic medium layers was solved by the modified Ambartsumyan method for the summation of layers [7, 11, 12]. The problems of such a character can also be solved by other methods (transfer matrix method, Jones matrix method, etc.). Let us note that a new method for solving the problems of light passage through a one-dimensional system was proposed in [13, 14].

The ordinary and extraordinary refractive indices of CLC sublayers are as follows: $n_o = \sqrt{\varepsilon_2} = 1.4639$ and $n_e = \sqrt{\varepsilon_1} = 1.5133$. These are the parameters of a CLC layer of the composition cholesteryl nonanoate : cholesteryl chloride : cholesteryl acetate = 20 : 15 : 6; at room temperature (24°C), it has a pitch of helix $p = \pm 420$ nm in the optical region and exhibits diffraction reflection for normal incidence of light in the wavelength range 615–635 nm. Here, ε_1 and ε_2 are the principal values of the permittivity tensor of CLC, and the CLC sublayer spiral is right-handed. Moreover, the first sublayer of the system is assumed to be an isotropic medium layer, and its refractive index is n_0.

Figure 2 shows the reflectance spectrum for one of the orders of diffraction reflection. The light incident on the system has the polarization that coincides with the first ($i = 1$, almost left circular polarization, dashed line) and the second ($i = 2$, almost right-hand circular polarization, solid line) eigenpolarization (EP). Eigenpolarizations (EPs) are two incident wave polarizations that do not change when light propagates through a system. EPs give much information on the interaction of light with a system; therefore, the calculation of EP for every optical system is important in optics and photonics. As follows from the definition of EPs, they should be related to the polarizations of the internal waves (eigenmodes) excited in a medium (they mainly coincide with the polarizations of eigenmodes). In particular, the authors of [6] showed that EPs are almost orthogonal at an odd number of sublayers in the system and are quasi-orthogonal at an even number of sublayers in the system, and the moduli of the ellipticity of EPs differ substantially from unity in selective reflection regions (see below).

As is seen from Fig. 2, the following three PBGs form for each order of diffraction reflection: one PBG is nonselective with respect to the polarization of incident light, and two others are selective. The Bragg conditions for these three band gaps have the form

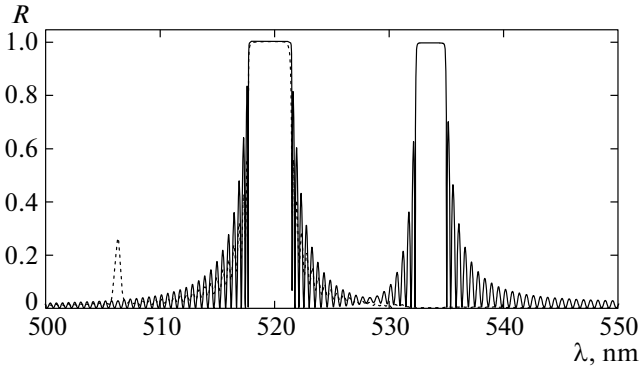

Fig. 2. Reflectance spectrum of the system for one of the orders of diffraction reflection under normal incidence. The light incident on the system has polarization that coincides with the first (dashed curve) and second (solid curve) EP. $d_1 = 500$ nm, $d_2 = 1000$ nm, $n_0 = 1.7$, and $s = 200$.

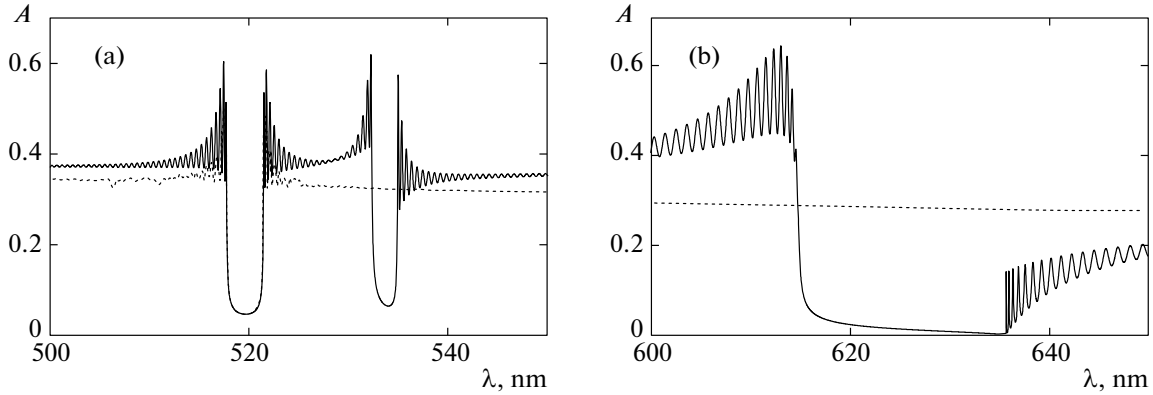

Fig. 3. Absorption spectra for normal incidence of light for (a) stack consisting of CLC and isotropic medium layers and (b) homogeneous CLC layer of thickness $sd_2/2$. The light incident on the system has polarization that coincides with the first (dashed curve) and second (solid curve) EP. $d_1 = 500$ nm, $d_2 = 1000$ nm, $n_0 = 1.7$, $s = 200$, $\mathrm{Im}\varepsilon_1 = 0$, and $\mathrm{Im}\varepsilon_2 = 0.001$.

$$d_2\bar{n} + d_1 n_0 = m\frac{\lambda}{2} \text{ for first-type PBG}, \quad (1)$$

$$d_2 n_1 + d_1 n_0 = m\frac{\lambda}{2} \text{ for second-type PBG}, \quad (2)$$

$$d_2 n_2 + d_1 n_0 = m\frac{\lambda}{2} \text{ for third-type PBG}, \quad (3)$$

where m is an integer; d_2 and d_1 are the sublayer thicknesses of CLC and the isotropic medium, respectively,

$$\bar{n} = \sqrt{\frac{\varepsilon_1 + \varepsilon_2}{2}}, \quad n_{1,2} = \bar{n}\sqrt{1 + \chi^2 - \delta \pm \sqrt{4\chi^2 + \delta^2}},$$

$$\delta = \frac{\varepsilon_1 + \varepsilon_2}{\varepsilon_1 - \varepsilon_2}, \quad \chi = \frac{\lambda}{p\bar{n}},$$

and p is the pitch of CLC helix.

To minimize the influence of dielectric boundaries, we perform calculations for a stack bounded by half-space with refractive index $n_s = \bar{n}$ on either side.

The diffraction efficiency of third-type PBG is usually very weak and manifests itself only at large system thicknesses. The frequency width of PBG depends on the corresponding harmonic in the Fourier series of the effective permittivity tensor of the system. Our investigations demonstrate that the maximum frequency width of first-type PBG is proportional to anisotropy $|\bar{n} - n_0|$ and the maximum frequency width of second-type PBG is proportional to the local anisotropy of the CLC sublayers. The frequency width of PBG also depends on the optical thickness of the structure sublayers (see [6–10] for details).

It follows from Eqs. (1)–(3) and the aforesaid that the photonic band structure of the system can be controlled by choosing the isotropic sublayer parameters.

The introduction of isotropic sublayers into a CLC matrix also changes the distribution of light field in the system. Therefore, in the general case, the effect of almost full suppression of absorption and the effect of anomalously strong absorption, which was observed in a finite CLC layer near PBG boundaries during anisotropic absorption, cannot be observed. (Absorption can be fully suppressed only at an infinite CLC layer thickness.) Indeed, Fig. 3 shows absorption spectra $A = 1 - (R + T)$, where R is the reflection coefficient and T is the transmission coefficient, for the structure under study (Fig. 3a) and a finite CLC layer of thickness $sd_2/2$ (Fig. 3b). It is seen that absorption is almost fully suppressed in the case of a homogeneous CLC layer at the short-wavelength PBG boundary and that anomalous is anomalously strong at the long-wavelength boundary. These effects are much weaker for the case of a stack of CLC and isotropic medium layers.

However, we will show below that these effects can also manifest themselves in the system under study if certain conditions are imposed on the sublayer thickness in the isotropic medium.

PCs are widely used as a laser cavity. Laser generation in a finite CLC layer was experimentally detected in [15, 16]. Laser generation in a finite CLC layer and multilayer structures with CLC layers is being extensively studied [17–29].

The photonic density of states (PDS), i.e., the number of modes per unit frequency range, is the most important PC characteristic. PDS is a quantity reciprocal to group velocity and can be expressed through the real and imaginary parts of transmission amplitude [30],

$$\rho_i(\omega) \equiv \frac{dk_i}{d\omega} = \frac{1}{d}\frac{\dfrac{du_i}{d\omega}\nu_i - \dfrac{d\nu_i}{d\omega}u_i}{u_i^2 + \nu_i^2}, \quad i = 1, 2, \quad (4)$$

where d is the system thickness and u_i and ν_i are the real and imaginary parts of transmission amplitude $T_i(\omega) = u_i(\omega) + i\nu_i(\omega)$. Relative PDS $\rho_i(\omega)/\rho_{\mathrm{iso}}$, where $\rho_{\mathrm{iso}} = n_s/c$, is usually calculated. It is important to cal-

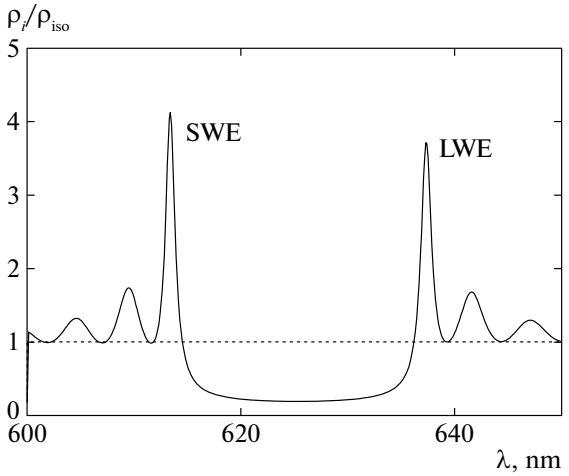

Fig. 4. ρ_i/ρ_{iso} spectrum for a finite CLC layer. The CLC layer thickness is $d = 50p$ and $n_s = \overline{n}$. The light incident on the system has left- (dotted line) and right-hand (solid curve) circular polarization.

culate PDS also due to the fact that many optical properties are expressed in terms of PDS. In particular, according to the Fermi golden rule, the luminescence intensity is proportional to PDS, and threshold gain g_{th} can be also expressed in terms of PDS, $g_{th} \propto n_s/d\rho$ [28]. It was theoretically and experimentally shown [15, 20, 21, 23, 24] that PDS for a finite CLC layer has two principal maxima at PBG boundaries, so-called short-wavelength (SWM) and long-wavelength (LWM) maxima (see Fig. 4).

Figure 5 shows the $\rho_i(\omega)/\rho_{iso}$ spectra of two EPs for the system under study at the parameters of Fig. 3. It is seen that, at the PBG boundaries located near the PBG of a homogeneous CLC layer (i.e., near or in the range from 615 to 635 nm), PDS increases in a resonance manner at the boundaries corresponding to PBGs. Below, we will show that an additional significant increase in $\rho_i(\omega)/\rho_{iso}$ at the PBG boundaries located in the range 615–635 nm, almost full suppression of absorption, and anomalously strong absorption can be achieved by choosing a proper isotropic layer thickness.

The evolution of reflectance spectra caused by a change in isotropic sublayer thickness d_1 was studied in [6–8]. As follows from those works and the aforesaid, the frequency position and the frequency width of PBG are functions of the isotropic sublayer thickness (and the CLC sublayer thickness). As the isotropic sublayer thickness increases in the system, PBG of each order shifts toward long waves. Moreover, its frequency width changes: it increases and then decreases periodically. Figure 6 also depicts the evolution of reflectance spectra caused by a change in the isotropic sublayer thickness. Incident light has right- (a) and left-hand (b) circular polarization.

We now study the possibilities of full suppression of absorption and anomalously strong absorption of radiation near PBG boundaries during anisotropic absorption. Our investigations demonstrate that the effects of almost full suppression of absorption and anomalously strong absorption are detected during anisotropic absorption (in CLC sublayers) when the isotropic sublayer thickness is chosen so that the short-wavelength boundary of second-type PBG coincides with the short-wavelength PBG boundary from a homogeneous CLC layer or the long-wavelength boundary of second-type PBG coincides with the long-wavelength PBG boundary from a homogeneous CLC layer. The hit horizontal dashed lines in Fig. 6a indicate the PBG boundaries from a homogeneous CLC layer. The vertical lines illustrate the method of choosing one of the possible pairs of isotropic sublayer thicknesses such that the conditions described above are met.

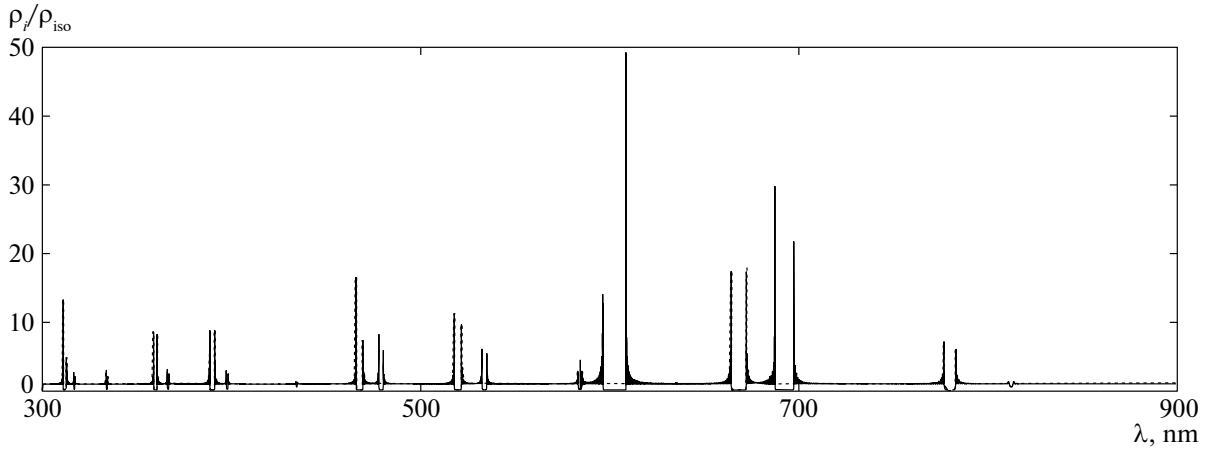

Fig. 5. $\rho_i(\omega)/\rho_{iso}$ spectra for normal light incidence for a stack of CLC layers and an isotropic medium. Absorption is absent. The other parameters are identical to those in Fig. 3.

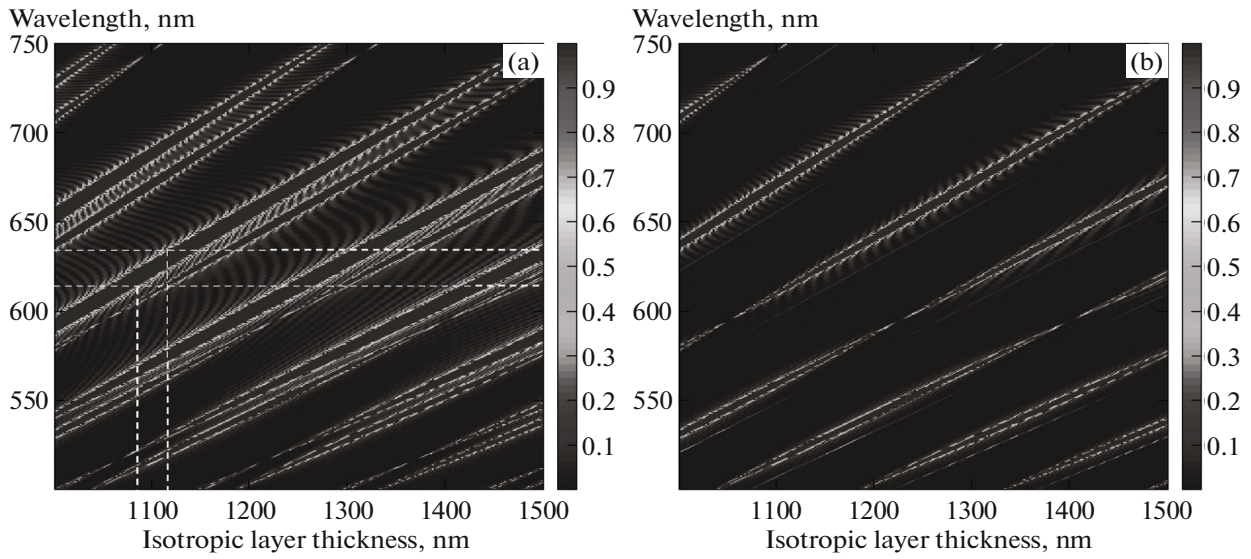

Fig. 6. Evolution of reflectance spectra as a function of the isotropic sublayer thickness. The parameters are identical to those in Fig. 3.

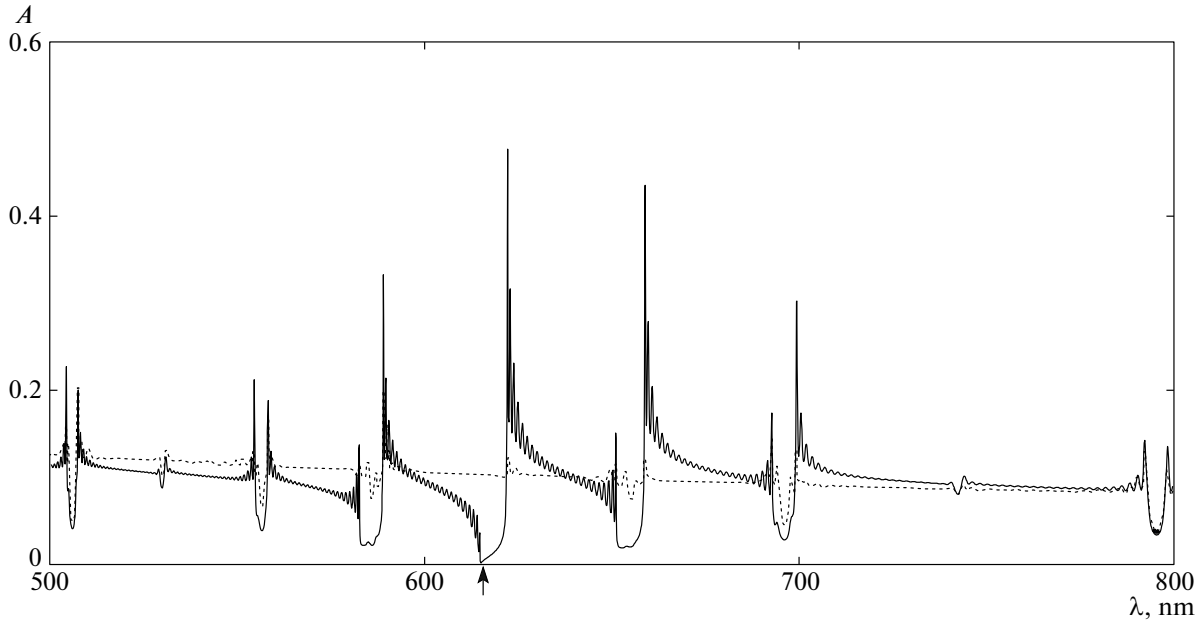

Fig. 7. Absorption spectrum for normal incidence of light for a stack consisting of CLC and isotropic medium layers. The light incident on the system has polarization that coincides with the first (dotted curve) and second (solid curve) EP. $d_1 = 2171$ nm, $d_2 = 3s$, $n_0 = 1.7$, $s = 50$, $\mathrm{Im}\varepsilon_1 = 0$, and $\mathrm{Im}\varepsilon_2 = 0.001$.

Figure 7 shows the absorption spectrum for the case where the short-wavelength boundary of second-type PBG for one of the orders of diffraction reflection coincides with the short-wavelength PBG boundary from a homogeneous CLC layer. It is seen that absorption is almost fully suppressed at the short-wavelength boundary of this PBG (indicated by the arrow). Figure 8 depicts the absorption spectrum for the case where the long-wavelength boundary of second-type PBG for one of the orders of diffraction reflection coincides with the long-wavelength PBG boundary from a homogeneous CLC layer. It is seen that absorption is almost fully suppressed at the long-wavelength boundary of this PBG (indicated by the arrow). It follows from these results that, under these conditions, the field distribution in the CLC sublayers is the same as in the homogeneous CLC layer and has

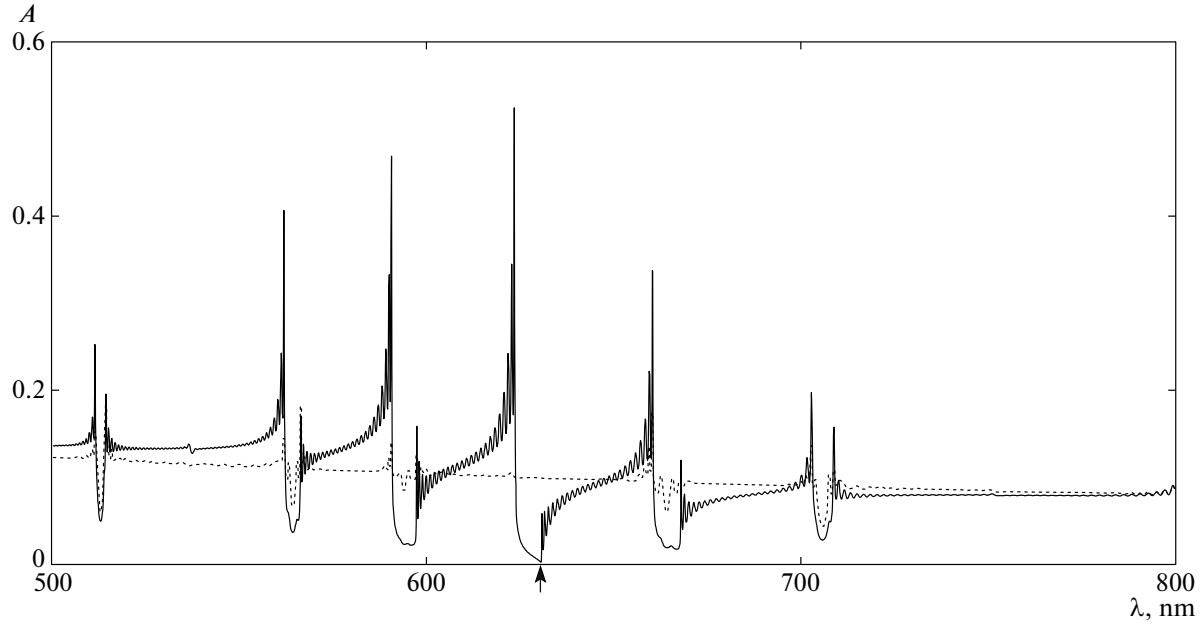

Fig. 8. Absorption spectrum for normal incidence of light for a stack consisting of CLC and isotropic medium layers. The light incident on the system has polarization that coincides with the first (dotted curve) and second (solid curve) EP. $d_1 = 2217$ nm, $d_2 = 3s$, $n_0 = 1.7$, $s = 50$, $\mathrm{Im}\varepsilon_1 = 0.001$, and $\mathrm{Im}\varepsilon_2 = 0$.

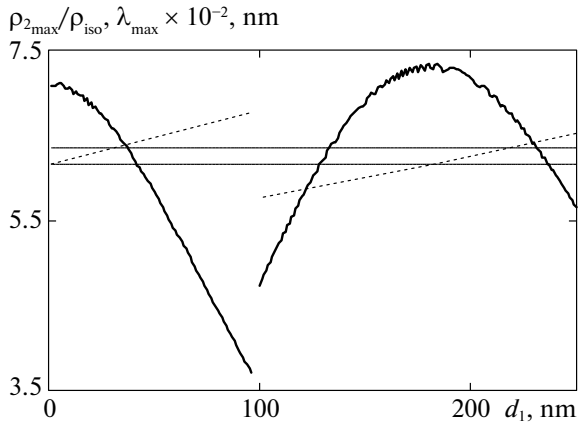

Fig. 9. $\rho_{2\max}/\rho_{iso}$ vs. the isotropic sublayer thickness: $d_2 = 1200$ nm and $s = 50$. The other parameters are identical to those in Fig. 2.

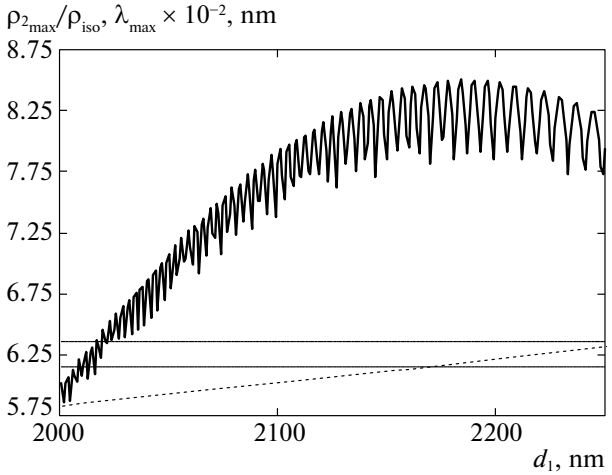

Fig. 10. $\rho_{2\max}/\rho_{iso}$ vs. the isotropic sublayer thickness. The parameters are identical to those in Fig. 9.

polarization peculiarities, which were described in detail, in particular, in [2, 29].

We now pass to studying the influence of fulfillment of these conditions on PDS. Figure 9 plots $\rho_{2\max}/\rho_{iso}$ versus the isotropic sublayer thickness. The horizontal lines indicate the PBG boundaries of a homogeneous CLC layer. The dashed lines illustrate $\lambda_{\max}$ versus the isotropic sublayer thickness ($\lambda_{\max}$ is the incident light wavelength at which $\rho_2/\rho_{iso} = \rho_{2\max}/\rho_{iso}$). It is seen that, when d_1 changes, $\rho_{2\max}/\rho_{iso}$ passes through a peak at the isotropic sublayer thickness such that the boundary of second-type PBG coincides with the short-wavelength boundary of PBG from a homogeneous CLC layer.

Figure 10 depicts the same dependence for another d_1 range. A comparison of these results with the analogous results in Fig. 9 demonstrates that the $\rho_{2\max}/\rho_{iso}$ oscillation amplitude increases with d_1 at large isotropic sublayer thicknesses.

We also studied the short- and long-wavelength $\rho_{2\max}/\rho_{iso}$ maxima as functions of CLC sublayer thickness d_2 for incident light with polarization coinciding

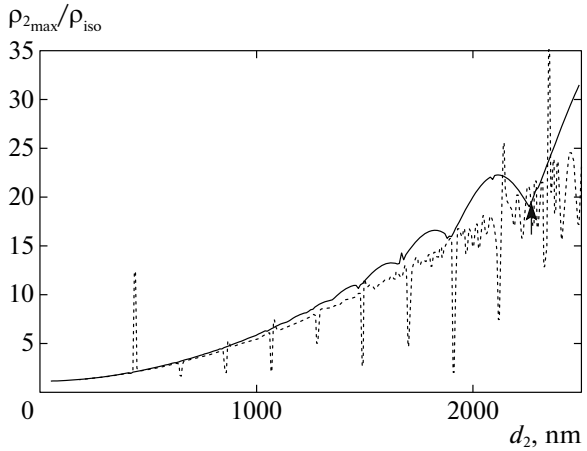

Fig. 11. Short- (solid curve) and long-wavelength (dotted curve) ρ_{2max}/ρ_{iso} maxima versus CLC sublayer thickness d_2. The parameters are identical to those in Fig. 9.

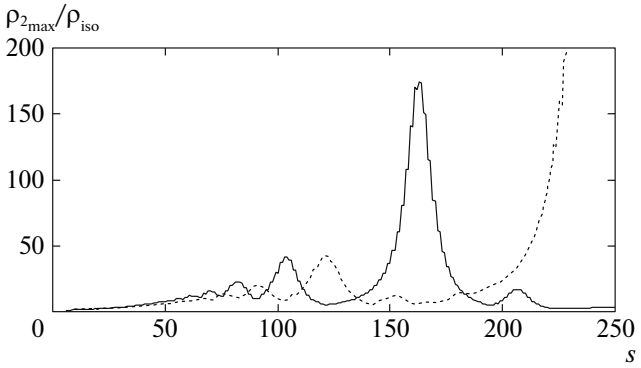

Fig. 12. Short- (solid curve) and long-wavelength (dotted curve) ρ_{2max}/ρ_{iso} maxima versus the system thickness (the number of sublayer parameters in the system s). The parameters are identical to those in Fig. 9.

with the second EP. Figure 11 plots the short- (solid curve) and long-wavelength (dotted curve) ρ_{2max}/ρ_{iso} maxima versus CLC sublayer thickness d_2. It is seen that, as d_2 increases, the short-wavelength ρ_{2max}/ρ_{iso} maximum first increases monotonically and then increases in an oscillating manner. At local oscillation minima, we have $d_2 = np/2$, where n is an integer (at such CLC sublayer thicknesses, ρ_{2max}/ρ_{iso} undergoes jumplike changes).

Finally, we studied the effect of the system thickness on the short- and long-wavelength ρ_{2max}/ρ_{iso} maxima. Figure 12 plots the short- (solid curve) and long-wavelength (dotted curve) ρ_{2max}/ρ_{iso} maxima versus the system thickness (the number of sublayers in the system s). It is seen that ρ_{2max}/ρ_{iso} increases monotonically with s at low values of s and begins to oscillate at a variable amplitude when s increases further. This behavior means that the number of sublayers in the system begins important to obtain high values of ρ_{2max}/ρ_{iso} at large thicknesses.

3. CONCLUSIONS

Some new peculiarities of the reflectance spectra of a stack consisting of CLC and isotropic medium layers are studied. The soft character of CLCs makes it impossible to form homogeneous thick layers, which is an important condition for some applications of CLC layers, in particular, when a CLC layer is applied as a laser cavity. We propose to introduce equidistant layers of isotropic media processed in a certain manner into a CLC matrix. This new system is known to acquire new properties: in particular, it has multicolor reflection. In the general case, however, this system loses a number of important properties of a homogeneous CLC layer. We showed that, under certain resonance conditions, this system can exhibit all well-known and useful properties of both a homogeneous CLC layer and a stack consisting of a CLC and isotropic medium layers. Here, some conditions are only imposed on the isotropic sublayer thickness. If these isotropic layers are assumed to be made of transparent materials, the ability to control the system parameters using an external longitudinal (and transverse) electric field increases. As was noted above, the possibility of controlling the parameters of a system over wide limits is the most important problem in photonics. From this standpoint, the proposed system is promising.

REFERENCES

1. E. I. Kats, Sov. Phys. JETP **33** (3), 634 (1971).
2. V. A. Belyakov, *Diffraction Optics of Complex Structured Periodic Media* (Springer-Verlag, New York, 1992).
3. N. Y. Ha, Y. Ohtsuka, S. M. Jeong, S. Nishimura, G. Suzaki, Y. Takanishi, K. Ishikawa, and H. Takezoe, Nat. Mater. **7**, 43 (2008).
4. E. M. Nascimento, I. N. de Oliveira, and M. L. Lyra, J. Appl. Phys. **104** (10), 103511 (2008).
5. Z. He, Z. Ye, Q. Cui, J. Zhu, H. Gao, Y. Ling, H. Cui, J. Lu, X. Gao, and Y. Su, Opt. Commun. **284** (16–17), 4022 (2011).
6. M. Z. Harutyunyan, A. H. Gevorgyan, and G. K. Matinyan, Opt. Spectrosc. **114** (4), 601 (2013).
7. A. H. Gevorgyan and G. K. Matinyan, J. Exp. Theor. Phys. **118** (5), 771 (2014).
8. A. H. Gevorgyan, G. K. Matinyan, M. Z. Harutyunyan, and E. M. Harutyunyan, J. Phys.: Conf. Ser. **517**, 012033 (2014).
9. A. H. Gevorgyan, M. Z. Harutyunyan, G. K. Matinyan, and S. A. Mkhitaryan, J. Phys.: Conf. Ser. **517**, 012034 (2014).
10. K. B. Oganesyan, A. H. Gevorgyan, A. N. Kocharian, G. A. Vardanyan, Yu. S. Chilingaryan, E. A. Santrosyan, and Y. V. Rostovtsev, Proc. SPIE **9182**, 918218 (2014).

11. A. H. Gevorgyan, Phys. Rev. E: Stat., Nonlinear, Soft Matter Phys. **83**, 011702 (2011).
12. A. H. Gevorgyan and M. Z. Harutyunyan, Phys. Rev. E: Stat., Nonlinear, Soft Matter Phys. **76**, 031701 (2007).
13. L. B. Glebov, J. Lumeau, S. Mokhov, V. Smirnov, and B. Ya. Zeldovich, J. Opt. Soc. Am. A **25**, 751 (2008).
14. S. Mokhov and B. Ya. Zeldovich, Proc. R. Soc. London, Ser. A **464**, 3071 (2008).
15. I. P. Il'chishin, E. A. Tikhonov, V. G. Tishchenko, and M. T. Shpak, JETP Lett. **32** (1), 24 (1980).
16. V. I. Kopp, B. Fan, H. K. M. Vithana, and A. Z. Genack, Opt. Lett. **23** (21), 1707 (1998).
17. L. M. Blinov, *Liquid Crystal Microlasers*, Ed. by R. Bartolino (Transworld Research Network, Trivandrum, Kerala, India, 2010).
18. H. Coles and S. Morris, Nat. Photon. **4**, 676 (2010).
19. V. A. Belyakov, Mol. Cryst. Liq. Cryst. **453**, 43 (2006).
20. A. H. Gevorgyan and M. Z. Harutyunyan, J. Mod. Opt. **56**, 1163 (2009).
21. A. H. Gevorgyan, K. B. Oganesyan, E. M. Harutyunyan, and S. O. Arutyunyan, Opt. Comm. **283** (19), 3707 (2010).
22. Y. Matsuhita, Y. Huang, Y. Zhou, Sh-T. Wu, R. Ozaki, Y. Takao, A. Fujii, and M. Ozaki, Appl. Phys. Lett. **90** (9), 091114 (2007).
23. Th. K. Mavrogordatos, S. Morris, F. Castles, P. J. W. Hands, A. D. Ford, H. J. Coles, and T. D. Wilkinson, Phys. Rev. E: Stat., Nonlinear, Soft Matter Phys. **86** (1), 011705 (2012).
24. A. Muñoz, M. E. McConney, T. Kosa, P. Luchette, L. Sukhomlinova, T. J. White, T. J. Bunning, and B. Taheri, Opt. Lett. **37** (14), 2904 (2012).
25. Th. K. Mavrogordatos, S. M. Morris, S. M. Wood, H. J. Coles, and T. D. Wilkinson, Phys. Rev. E: Stat., Nonlinear, Soft Matter Phys. **87** (6), 062504 (2013).
26. P. V. Dolganov, Phys. Rev. E: Stat., Nonlinear, Soft Matter Phys. **91** (4), 042509 (2015).
27. A. H. Gevorgyan, K. B. Oganesyan, R. V. Karapetyan, and M. S. Rafayelyan, Laser Phys. Lett. **10** (12), 125802 (2013).
28. M. F. Moreira, S. Relaix, W. Cao, B. Taheri, and P. Palffy-Muhoray, in *Liquid Crystal Microlasers*, Ed. by R. Bartolino (Transworld Research Network, Trivandrum, Kerala, India, 2010).
29. A. H. Gevorgyan, K. B. Oganesyan, G. A. Vardanyan, and G. K. Matinyan, Laser Phys. **24** (11), 115801 (2014).
30. J. M. Bendickson, J. P. Dowling, and M. Scalora, Phys. Rev. E: Stat. Phys., Plasmas, Fluids, Relat. Interdiscip. Top. **53** (4), 4107 (1996).

Translated by K. Shakhlevich